Superluminescence in InAsSb circular-ring-mode light-emitting diodes for CO gas detection

V. V. Sherstnev and A. M. Monahov
Ioffe Physico-Technical Institute, St. Petersburg, 195279, Russia

A. Krier[a)]
Physics Department, Lancaster University, Lancaster, LA1, 4YB, United Kingdom

G. Hill
III–V Central Facility, Electronic and Electrical Engineering Department, University of Sheffield, Mappin Street, Sheffield, S1 3JD, United Kingdom

(Received 19 June 2000; accepted for publication 26 October 2000)

We report on the superluminescence of an InAsSb light-emitting diode, operating at 4.6 μm, suitable for carbon monoxide gas detection. The source is based on an optical whispering (or circulating) mode which is generated near the edges of the mesa and which is responsible for the superluminescence. A pulsed optical output power in excess of 2.2 mW at room temperature has been measured, making these emitters suitable for use in cost-effective instruments for the environmental monitoring of carbon monoxide at 4.6 μm. © *2000 American Institute of Physics.* [S0003-6951(00)04151-6]

The midinfrared (2–5 μm) spectral range contains the strong fundamental molecular absorption bands of a number of combustible and atmospheric pollutant gases. Currently, infrared gas detection techniques based on optical absorption are becoming increasingly popular as they are the only ones, which are truly gas specific and therefore reliable for gas sensor instrumentation.[1,2] Consequently, there has been much research interest aimed at providing monochromatic sources suitable for gas analysis and detection, such that a number of midinfrared light-emitting diodes (LEDs) operating at different target wavelengths have been realized.[3–6]

Nonradiative recombination is a significant problem in narrow gap III–V semiconductor light sources and both Auger and Shockley–Read–Hall recombination processes can limit the internal quantum efficiency and output power. Until now, this has prevented the practical application of these LEDs in gas sensor instrumentation. Previously, we reported on the fabrication of a LED for CO detection with an optical output power of 50 μW (Ref. 7) and subsequently, by using a rare earth gettering technique[8] to purify the active region, an improved device with a pulsed output power in excess of 1 mW has been achieved.[9] The increase in optical output power in our recent investigations has come about largely through a careful reduction of the residual carrier concentration in the active region of mesa etched LEDs with a central dot contact. In this letter, we report on the fabrication of a superluminescent LED with a ring contact which produces a circular waveguide due to current crowding effects. A whispering gallery mode is generated as injection is increased, resulting in superluminescence and a 300 K LED with an optical output power in excess of 2.2 mW at 4.6 μm.

The LEDs were all fabricated from III–V double heterostructures grown by liquid phase epitaxy (LPE). A conventional horizontal, multiwell graphite sliding boat was used for the LPE growth of the LED structures onto *n*-type InAs (100) substrates. These were 14 mm$\times$14 mm square with a carrier concentration of $1\times10^{18}\,cm^{-3}$ and were obtained from Wafer Technology Ltd. The LED structure, which has been described in detail previously elsewhere,[7] consists of two cladding layers of N–InAsSbP and P–InAsSbP and an undoped active region of $InAs_{0.89}Sb_{0.11}$ sandwiched between them. Because the $InAs_{0.89}Sb_{0.11}$ ternary active region material has a large lattice mismatch with respect to the InAs substrate layer, a buffer layer, with an intermediate composition of $InAs_{0.94}Sb_{0.06}$ and having a 0.41% positive mismatch to the InAs substrate layer, was introduced between the substrate and the N-type InAsSbP layer in order to reduce dislocations and to relieve strain caused by the lattice mismatch.

The buffer layer was heavily doped (*n* type) with Te up to $4\times10^{18}\,cm^{-3}$ and was 4 μm in thickness. The quaternary cladding layers were doped to $1\times10^{17}\,cm^{-3}$ *n* type and $2\times10^{17}\,cm^{-3}$ *p* type, respectively. The resulting epitaxial structures were processed using conventional photolithography, but two different types of LED chips were fabricated for comparison. For the first type (LED I) mesa diodes were fabricated from the patterned epitaxial wafers by dry plasma etching using CH_4:H_2 to produce round mesas 420 μm in diameter (emitting area $1.39\times10^{-3}\,cm^2$). The mesa surface was then passivated using Si_3N_4. A Nomarski microscope photograph of a typical mesa etched (LED I) chip produced in this way is shown in Fig. 1. For the second type of device (LED II) square chips of dimensions 450 μm$\times$450 μm (with emitting area $1.94\times10^{-3}\,cm^2$) were defined, again using photolithography, and were etched out, but this time using wet chemical etching and without forming a mesa structure. The ohmic top contact which was employed was the same for both types of devices and was produced in the form of a ring contact which was 300 μm in diameter and 30 μm wide. The corresponding back contact was deposited over the en-

a)Electronic mail: a.krier@lancaster.ac.uk

 © 2000 American Institute of Physics

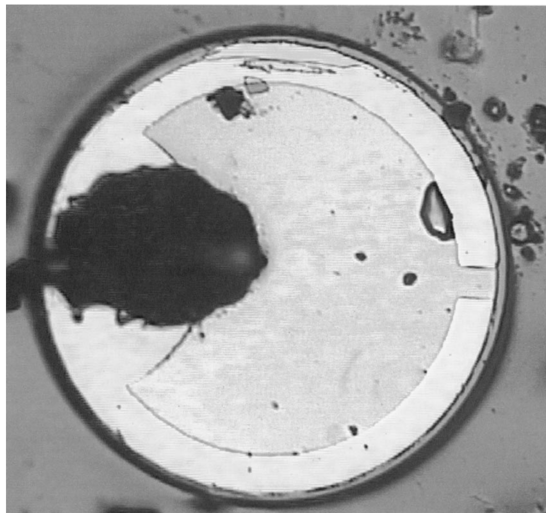

FIG. 1. Nomarski microscope photograph of LED I.

tire rear surface of the chip. Each of the contacts was deposited by thermal evaporation of Au:Zn alloy+Au on the *p* side and Au:Te alloy+Au on the *n* side of the diode, respectively. Once the LED chips had been prepared, they were mounted onto standard TO49 packages using Ag epoxy. Before testing, they were also equipped with a small parabolic reflector which was attached to the TO-49 header in order to help focus the LED output in the forward direction. The full width at half maximum (FWHM) of the resulting output beam obtained with this arrangement (for each LED type) was about 12°. Since the LED chip was effectively placed at the focus of a parabola, the output beam was focused to a small spot (<1 mm diam.) at a distance about 40 mm away, which is near optimal for many gas sensor instrument applications.

Figure 2 shows the electroluminescence emission spectra of the mesa etched LED I measured with increasing drive current. The distinctive feature of these spectral curves is

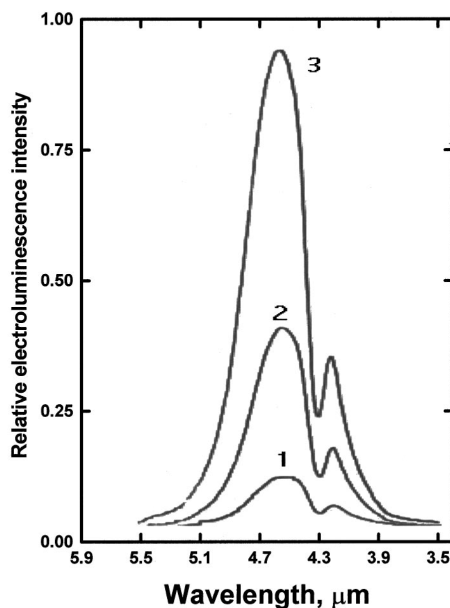

FIG. 2. The room-temperature electroluminescence emission spectrum obtained from LED I, measured at increasing drive currents: 15 mA (curve 1), 50 mA (curve 2), and 100 mA (curve 3) at 560 Hz using a 50% duty cycle.

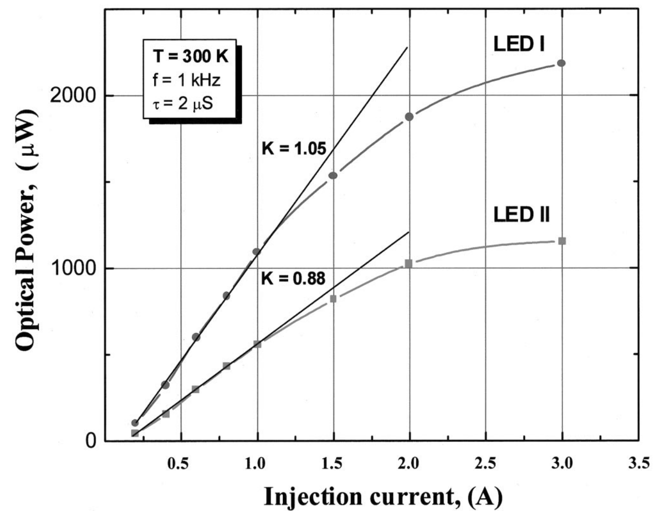

FIG. 3. Light–current characteristics measured from the 2 different LEDs. LED I is a mesa etched LED chip with a diameter of 420 μm, LED II is 450×450 μm square. Both LEDs were fabricated with a ring contact 300 μm in diameter. The characteristics were measured at room temperature at currents from 0.2 to 3.0 A in the pulsed regime with a 1 kHz frequency using a 0.2% duty cycle (2.0 μs pulses).

their decreasing linewidth with increasing current. The halfwidth (FWHM) of the line at 15 mA is 880 nm whereas at 100 mA it is only 580 nm. The ratio of these halfwidths is 1.51. This spectral behavior shows that the device under consideration is a superluminescent diode. LED II also exhibited some line narrowing in the electroluminescence spectrum but the ratio of the halfwidths under the same drive conditions was only 1.17. The dip near 4.2 μm is due to CO_2 absorption from the atmosphere. The optical output power was also measured for the two different devices with a pulse duration of 2 μs at a repetition rate of 1 kHz in the current range from 0.2 to 3 A. The resulting optical output–current relationships are compared in Fig. 3. Both the curves have a linear portion in the current range from 0.2 to 1 A. The corresponding slopes were determined to be 1.05 for LED I and 0.88 for LED II. A value of the slope of the light–current characteristic which is greater than 1 is further evidence for superluminescence in LED I.

The above results demonstrate that LED I operates as a superluminescent diode unlike LED II. The LED I device has a ring contact with external and internal diameters much larger than the active layer thickness. The conductivity of the upper gold ring contact and the heavily doped n^+ layer (and certainly the lower contact) are at least two orders of magnitude higher than the conductivity of the active layer. One can estimate the resulting current density distribution in the active layer by considering, as a model, a conductive layer between an infinite metal plate and a metal ring.[10] The current density distribution on the lower plate is given by (units are chosen so that the layer width is a unit of length and the coefficient before the integral is equal to 1);

$$j_Z(R)=\int_{r_1}^{r_2}\frac{E\left(\frac{4Rx}{1+(R-x)^2}\right)}{(1+(R-x)^2)^{3/2}}\,dx, \qquad (1)$$

where r_1 and r_2 are the internal and external radii of the ring,

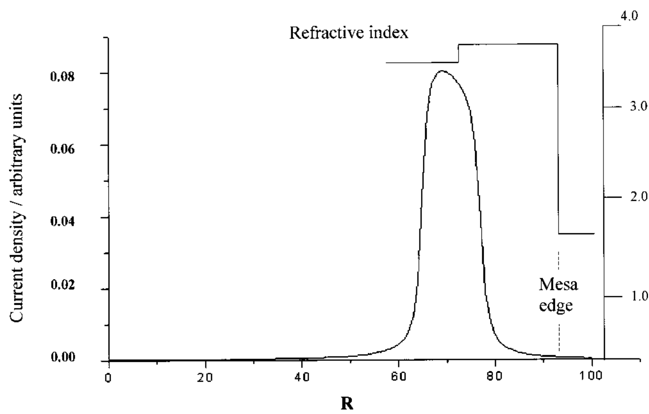

FIG. 4. Current density distribution in the lower plane obtained from Eq. (1). (The contact internal diameter in our units is 60 and the external diameter is 80.)

R is the distance from the center of the ring to the point of observation, and E is the complete elliptic integral;

$$E(x) = \int_0^{\pi/2} (1 - x \sin^2 \theta)^{1/2} d\theta.$$

A plot of the resulting current density distribution is shown in Fig. 4 and from which current crowding in the p-type material under the ring electrode is evident. Because of the increased carrier concentration the refractive index is reduced[11] and a circular ring waveguide arises between the ring and the edge of the mesa. The resulting refractive index profile is also shown schematically in Fig. 4. Consequently, the optical gain is locally higher near the edge of the mesa than in the rest of sample. This is of course the same for both LED I and LED II. However, the optical output power difference between LED I and LED II is due to the fact that the round mesa in LED I can support a circulating/whispering gallery mode much more easily. We also note that passivation of the mesa edge prevents the formation of an oxide which can produce a surface inversion layer. Consequently, the optical gain in this device is higher than in the square device without passivation.

Similar optical resonant mode behavior has been observed in microdisk lasers[12,13] and LEDs operating at much shorter wavelengths.[14,15] It has been shown that such a microdisk cavity may support two different resonant mode types, radial and whispering gallery modes (WG).[16] Radial modes are dominated by photon wave motion along the radial direction of the disk, the equivalent cavity being formed between the edge and the center of the disk. These radial oscillations are unlikely, in our case, due to the ring contact and local current crowding which prevents such propagation. The WG mode, on the other hand, may be thought of as in-plane propagation around the inside perimeter of the disk, or mesa in our case, which is facilitated by total internal reflection. The modes are solutions of the three-dimensional Maxwell equations. If, however, we assume that the radiation is effectively confined vertically within the active region of our mesa, then we may approximate this situation using a two dimensional solution which yields Bessel function solutions for the radial field distribution. The effective cavity length of $2\pi R$ imposed by the periodic boundary condition on the circulating wave results in the WG eigenmode condition: $2\pi Rn = m\lambda$ for large integer m, where R is the mesa radius, n is the refractive index, and the mode spacing is simply given by $\Delta\lambda_{WG} = \lambda^2/2\pi Rn$. This enables us to estimate a WG mode spacing of 4.6 nm which was too small for us to resolve with our low resolution spectrometer as is evident from the spectra of Fig. 2. Lasing is inhibited by the Q spoiling effect of the rough circumference of the mesa. But, higher order modes are less affected since their intensity maxima reside further away from the perimeter, while the ring contact suppresses the modes in the central area of the device. Although the parabolic reflector collects light emitted at low angles, further measurements showed that light was emitted from both the surface and the edges of the mesa.

In summary, we have observed superluminescence in the midinfrared at 4.6 μm from a mesa etched LED. Spectral line narrowing was observed and the optical output power of these diodes was found to be more than two times greater than that of analogous diodes of a different configuration. The superluminescence was due to optical resonant mode behavior which we attribute to high order whispering gallery modes, previously not reported in LEDs operating at wavelengths as long as 4.6 μm. This result suggests the possibility of creating a whispering gallery mode semiconductor laser working at room temperature in the spectral range 3–5 μm.

The authors wish to thank EPSRC for the award of a visiting fellowship for V.V.S. One of the authors (A.M.) would like to thank the Ministry of Science of the Russian Federation for partial support of this work through the program ''Optics and Laser Physics.''

[1] S. McCabe and B. D. MacCraith, Electron. Lett. **29**, 1719 (1993).
[2] S. D. Smith, A. Vass, P. Bramley, J. G. Crowder, and C. H. Wang, IEE Proc.-J: Optoelectron. **144**, 266 (1997).
[3] M. K. Parry and A. Krier, Electron. Lett. **30**, 1968 (1994).
[4] A. A. Popov, V. V. Sherstnev, Y. P. Yakovlev, A. N. Baranov, and C. Alibert, Electron. Lett. **33**, 86 (1997).
[5] A. Krier and Y. Mao, IEE Proc.-J: Optoelectron. **144**, 355 (1997).
[6] A. A. Popov, M. V. Stepanov, V. V. Sherstnev, and Y. P. Yakovlev, Tech. Phys. Lett. **24**, 596 (1997).
[7] H. H. Gao, A. Krier, and V. V. Sherstnev, J. Phys. D **32**, 1768 (1999).
[8] A. Krier, H. H. Gao, and V. V. Sherstnev, J. Appl. Phys. **85**, 8419 (1999).
[9] A. Krier, H. H. Gao, V. V. Sherstnev, and Y. Yakovlev, Electron. Lett. **35**, 1665 (1999).
[10] W. K. H. Panofsky and M. Phillips, *Classical Electricity and Magnetism* (Addison–Wesley, Reading, MA, 1960).
[11] P. P. Paskov, J. Appl. Phys. **81**, 1890 (1997).
[12] S. A. Backes, J. R. A. Cleaver, A. P. Heberle, J. J. Baumberg, and K. Kohler, Appl. Phys. Lett. **74**, 176 (2000).
[13] S. Chang, B. N. B. Rex, R. K. Chang, G. Chong, and L. J. Guido, Appl. Phys. Lett. **75**, 166 (2000).
[14] S. X. Jin, J. Li, J. Z. Li, J. Y. Lin, and H. X. Jiang, Appl. Phys. Lett. **76**, 631 (2000).
[15] R. A. Mair, K. C. Zeng, J. Y. Lin, H. X. Jiang, B. Zhang, L. Dai, A. Botchkarev, W. Kim, H. Morkoc, and M. A. Khan, Appl. Phys. Lett. **72**, 1530 (1998).
[16] R. P. Wang and M. M. Dumitrescu, J. Appl. Phys. **81**, 3391 (1997).